translation initiation complexes, while P-bodies are mRNP aggregates with proteins involved in mRNA decay and translational repression (2, 21). YB-1 accumulates in these cytoplasmic structures (2) and acts as either a translational activator or inhibitor depending on its amount bound to the target mRNP (55). Therefore, it is proposed that YB-1 determines the fate of cellular mRNPs from their synthesis to destruction.

Here, we found that YB-1 translocates to the nucleus in response to influenza virus infection. The YB-1 imported into the nucleus accumulates in nuclear speckles (promyelocytic leukemia nuclear bodies [PML NBs]), together with vRNP, M1, and NS2 in the presence of leptomycin B (LMB), a potent inhibitor of CRM1, suggesting that YB-1 is associated with the vRNP export complexes in the nucleus. At late phases of infection, YB-1 was found in perinuclear granules with the newly synthesized vRNP and accumulated in Rab11a-positive recycling endosomes along microtubules. Further, we found that YB-1 mediates the interaction of vRNP with microtubules. Taking these findings together, we propose that YB-1 functions as a porter that facilitates the association of the progeny vRNP with microtubules, thereby leading the travel of vRNP onto Rab11a-positivie recycling endosomes.

MATERIALS AND METHODS

Biological materials. vRNP was prepared from purified influenza A/Puerto Rico/8/34 (A/PR/8/34) virus as previously described (66). Rabbit polyclonal antibodies against YB-1, RAP55, RCK, PB1, PB2, PA, M1, and NP and rat antibody against NS2 were prepared as previously described (30, 31, 40, 50, 71, 72, 77). Rabbit polyclonal antibodies against TIAR, PML (Santa Cruz Biotechnology), and Rab11a (Invitrogen) and mouse monoclonal antibodies against α-tubulin (Sigma) and PML (Santa Cruz Biotechnology) were purchased. Anti-SeV antibody and anti-M1 monoclonal antibody were generous gifts from A. Kato (National Institute of Infectious Diseases, Japan) and S. Hongo and K. Sugawara (Yamagata University), respectively. MDCK, 293T, and HeLa cells were grown in minimal essential medium (MEM) containing 10% fetal bovine serum. For the construction of plasmids expressing His-YB-1 and FLAG-α-tubulin, the cDNAs were amplified with primers 5′-GGAATTCCATA TGAGCAGCGAGGCCGAGACCCAGC-3′ and 5′-GAACCGCTCGAGC TCAGCCCCGCCCTGCTCAGCCTCGGGAG-3′ for YB-1 and with primers 5′-CGCCACCATGGACTACAAGGATGACGACGACAAGCAT ATGCGTGAGTGCATCTCC-3′ and 5′-CTATTAATACTCTTCACCCT CAT-3′ for α-tubulin, and cDNAs were reverse transcribed from HeLa total RNA using oligo(dT)$_{20}$ primer as a template. YB-1 cDNA was cloned into plasmid pET24b, and the resultant plasmid was then used as a template to amplify FLAG-YB-1 cDNA with primers 5′-GCCGCCACCATG GACTACAAGGATGACGACGACAAGCATATGAGCAGCGAGGCCGA-3′ and 5′-CCCGGATCCTATTACTCAGCCCCGCCCTG-3′. FLAG-YB-1 and FLAG-α-tubulin cDNAs were cloned into plasmid pCAGGS. The cDNA fragments of YB-1 deletion mutants were amplified with primers 5′-GCAGATATCATGAGCAGCGAGGCCGA-3′ and 5′-TGCGGAT CCCTACCATGGCCCGCCGGCAGGC-3′ for the A/P domain (amino acids [aa]1 to 50), 5′-GCAGATATCATGAGCAGCGAGGCCGA-3′ and 5′-TGCGGATCCTTAACCAGGACCTGTAACATT-3′ for the ΔA/B domain (aa 1 to 129), 5′-GCAGATATCGACAAGAAGGTCATCGCAA-3′ and 5′-CCCGGATCCTATTACTCAGCCCCGCCCTG-3′ for the ΔA/P domain (aa 51 to 324), and 5′-GCACCATGGGATATCGGTGTTCCAG TTCAAGGC-3′ and 5′-CCCGGATCCTATTACTCAGCCCCGCCCT G-3′ for the A/B domain (aa 130 to 324) and then cloned into plasmid pGEX-6P. To establish HeLa cell lines constitutively expressing either FLAG-YB-1 or FLAG-α-tubulin, HeLa cells transfected with pSV2-Neo and either pCAGGS-FLAG-YB-1 or pCAGGS-FLAG-α-tubulin were selected by growth in the presence of 1 mg/ml G418 for 2 weeks, and then the G418-resistant colonies were isolated. Recombinant His-YB-1 and glutathione *S*-transferase (GST)-fused deletion mutants of YB-1 were purified according to the manufacturer's protocol. In addition, to remove the bacterial RNA possibly bound to YB-1, we treated recombinant YB-1 with RNase A before purification.

LC-MS analysis. Molecular masses of trypsin-digested peptides from proteins coimmunoprecipitated with NP were calculated by liquid chromatography-coupled mass spectrometry (LC-MS) analysis (Thermo) after reduction and alkylation of cysteine residues. Assignment of observed ions was done with Mascot search software.

Cellular localization of viral RNAs and proteins. Indirect immunofluorescence assays and fluorescence *in situ* hybridization (FISH) assays were carried out as previously described (28). Briefly, cells infected with A/PR/8/34 at multiplicity of infection (MOI) of 10 were fixed with 1% paraformaldehyde (PFA) for 5 min and then prepermeabilized with 0.01% digitonin in phosphate-buffered saline (PBS) for 5 min on ice. After being washed with PBS, cells were fixed in 4% PFA for 10 min and permeabilized with 0.5% Triton X-100 in PBS for 5 min on ice. After incubation in PBS containing 1% bovine serum albumin (BSA) for 1 h, coverslips were incubated with each antibody for 1 h and then with Alexa Fluor 488- or 568-conjugated anti-rabbit, -rat, and -mouse IgG antibodies (Invitrogen). After the indirect immunofluorescence assays, FISH assays were performed using RNA probes complementary to the segment 1 vRNA and cRNA/mRNA. Images were acquired by confocal laser scanning microscopy (Zeiss). Each micrograph is a confocal section taken at the same level of focus among samples, so that nuclei were fully observed with a maximum diameter.

Immunoprecipitation. Infected cells cross-linked with 0.5% formaldehyde for 10 min at room temperature were lysed by sonication in a buffer containing 20 mM Tris-HCl (pH 7.9), 100 mM NaCl, 30 mM KCl, 0.1% NP-40, and 1 mM EDTA. The lysates were subjected to centrifugation at 12,000 × *g*, and the supernatant fractions were subjected to immunoprecipitation with antibodies where indicated. For detection of viral RNAs immunoprecipitated with YB-1 from infected cells, the immunoprecipitates were subjected to reverse cross-linking in a buffer containing 50 mM Tris-HCl (pH 7.9), 5 mM EDTA, 50 mM dithiothreitol (DTT), and 1% SDS for 45 min at 70°C. After reverse cross-linking, viral RNAs were purified by phenol-chloroform extraction followed by ethanol precipitation and then reverse transcribed with primers to determine the levels of vRNA (5′-GACGATGCAACGGCTGGTCTG-3′, which corresponds to the segment 5 cRNA between nucleotide sequence positions 424 and 444), cRNA (5′-AGTAGAAACAAGGGTATTTTTCTTTA-3′, which is complementary to the segment 5 cRNA between nucleotide sequence positions 1540 and 1565), and viral mRNA [oligo(dT)$_{20}$ for poly(A) tail]. The synthesized single-stranded cDNAs were subjected to quantitative real-time PCR analysis (Dice real-time thermal cycler system TP800; TaKaRa) with two specific primers, i.e., 5′-GACGATGCAACGGCTGGT CTG-3′, which corresponds to the segment 5 cRNA between nucleotide sequence positions 424 and 444, and 5′-AGCATTGTTCCAACTCCTTT-3′, which is complementary to the segment 5 cRNA between nucleotide sequence positions 595 and 614.

Gene silencing mediated by siRNA. Short interfering RNAs (siRNAs) against the *Rab11a* and *YB-1* genes were purchased from Invitrogen. Cells (5×10^5) were transfected with 30 pmol of siRNA using Lipofectamine RNA interference (RNAi) Max (Invitrogen) according to the manufacturer's protocol.

Reconstruction of vRNP-microtubule complex mediated by YB-1. Cellular tubulin and microtubule-associated proteins (MAPs) purified from bovine brain as previously described (67) were kindly provided by K. Mizumoto (Kitasato University). The purified tubulin proteins (40 μg) were assembled into microtubules by incubation at 37°C for 20 min in a buffer containing 50 mM piperazine-*N*,*N*′-bis(2-ethanesulfonic acid) (PIPES)-NaOH (pH 6.8), 1 mM EGTA, 5 mM $MgCl_2$, 20% glycerol, 1 mM GTP, and 20 μM paclitaxel (originally named taxol). The reconstituted microtubules were precipitated by centrifugation at 32,000 rpm at 20°C for 20 min in an SW55Ti rotor (Beckman) to remove the monomeric

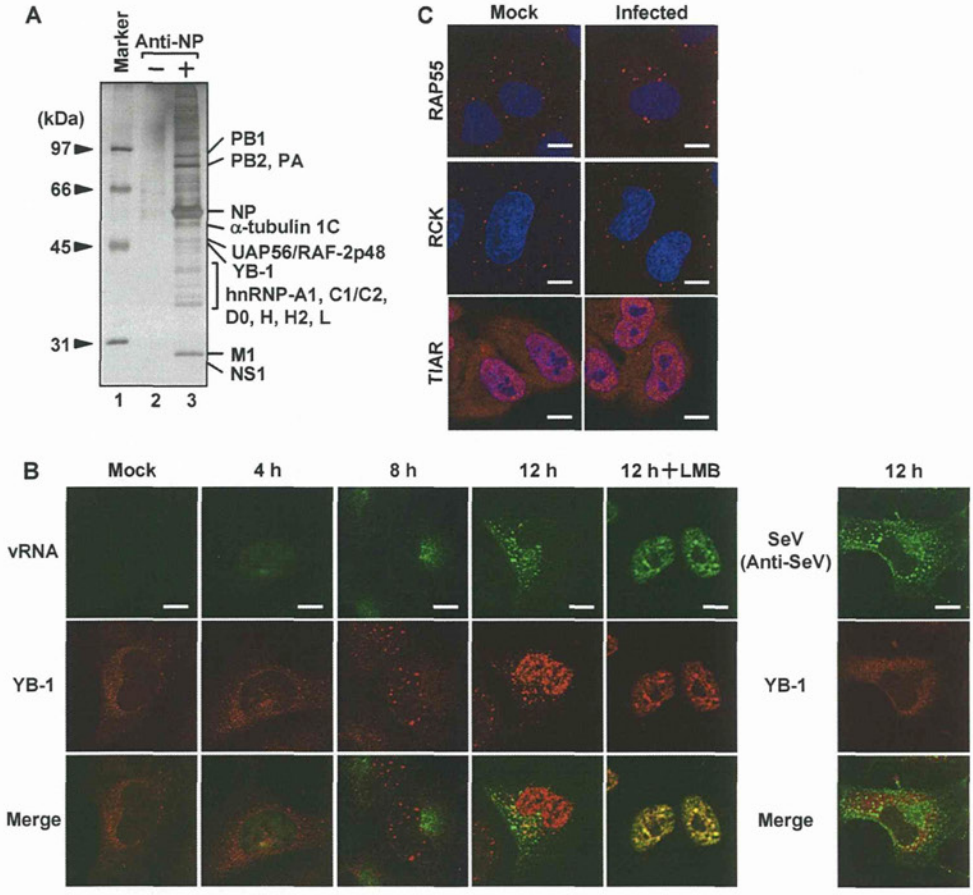

FIG 1 Identification of YB-1 as a novel vRNP-interacting proteins. (A) Identification of cellular and viral proteins interacting with vRNP complexes. HeLa cells infected with influenza virus at an MOI of 10 were subjected to immunoprecipitation assays with control IgG (lane 2) or anti-NP (lane 3) antibody-conjugated protein A-Sepharose. The coprecipitated proteins were eluted in 100 mM glycine (pH 2.8), separated through 10% SDS-PAGE, and visualized by silver staining. Molecular mass markers are also shown in lane 1. (B) Intracellular localization of YB-1 in infected cells. Infected MDCK cells were subjected to indirect immunofluorescence assays with anti-YB-1 antibody followed by FISH assays using a probe that hybridizes with segment 1 vRNA at 0, 4, 8, and 12 hpi. For LMB treatment, infected cells were incubated in culture medium containing 20 nM LMB at 7 hpi, and then the intracellular localization of vRNA and YB-1 was visualized by FISH and indirect immunofluorescence assays at 12 hpi. The result for SeV-infected cells at 12 hpi is also shown. Scale bars, 10 μm. (C) Intracellular localization of cellular proteins related to P-bodies and SGs. Mock-infected cells (left panels) or infected MDCK cells at 8 hpi (right panels) were subjected to indirect immunofluorescence assays with anti-RAP55 (upper panels, red), anti-RCK (middle panels, red), or anti-TIAR (lower panels, red) antibodies. Nuclear DNA was stained with TO-PRO-3 iodide (blue). Scale bars, 10 μm.

tubulin proteins. The precipitates were resuspended in a buffer containing 50 mM HEPES-NaOH (pH 7.9), 50 mM KCl, 20 μM paclitaxel, and 0.5% BSA and then incubated with either vRNP or YB-1-vRNP complexes. The vRNP complexes were immunoprecipitated with anti-NP antibody, and then the coprecipitated microtubules were detected by Western blotting assay with anti-α-tubulin antibody.

RESULTS

Identification of YB-1 as a novel vRNP-interacting protein. To gain further insight into the regulatory mechanism of vRNP function, we tried to identify a novel cellular protein(s) that interacts with vRNP. At 8 h postinfection (hpi), infected cell lysates were subjected to immunoprecipitation using anti-NP antibody, and then the precipitated proteins were subjected to LC-MS analysis (Fig. 1A). We found that viral proteins PB1, PB2, PA, M1, and NS1 were coprecipitated with NP, as expected (32, 39, 56, 58, 59), suggesting that not only NP but also vRNP was immunoprecipitated in this experiment. In addition to these viral proteins, we also identified a number of cellular proteins interacting with vRNP, as previously reported (Table 1) (29, 43, 44, 46, 76). It is noted that YB-1, a major component of cellular mRNP, was also identified as a novel vRNP-interacting protein. YB-1 regulates the lifetime and the translational activity of cellular mRNP, depending on the amount of YB-1 on a target mRNA (22, 55). Further, it is proposed that YB-1-bound mRNP particles interact with microtubules, but a precise role(s) of YB-1 has not yet been uncovered (11, 12). Thus, we tried to examine whether YB-1 regulates the fate of vRNP.

YB-1 localizes predominantly in the cytoplasm but translocates to the nucleus to regulate transcription in response to environmental stimuli such as DNA-damaging agents, UV irradiation, hyperthermia, and serum stimulation (34). More importantly, YB-1 is one of the components of SGs and P-bodies, which are cytoplasmic compartments possibly involved in the regulation of translation under stress conditions (78). Viral infection also gives a stressful environment to cells. To elucidate the biological significance of the interaction of vRNP with YB-1, we examined the

TABLE 1 LC-MS analysis of vRNP-interacting proteins

Protein	No. of observed peptides	Mascot score	Sequence coverage (%)
Heterogenous nuclear ribonucleoprotein A1	6	85	9
Heterogeneous nuclear ribonucleoproteins C1/C2	11	64	21
Heterogeneous nuclear ribonucleoprotein D0	4	77	12
Heterogeneous nuclear ribonucleoprotein H	9	159	17
Heterogeneous nuclear ribonucleoprotein H2	8	111	17
Heterogeneous nuclear ribonucleoprotein L	7	98	17
ATP-dependent RNA helicase DDX3Y	15	80	17
ATP-dependent RNA helicase DDX5	7	81	10
ATP-dependent RNA helicase DDX17	10	87	12
Nucleolin	8	85	13
78-kDa glucose-regulated protein	11	157	15
Importin subunit alpha 7	3	65	8
Y-box-binding protein 1	3	91	10
Tubulin alpha-1C chain	5	70	12
Spliceosome RNA helicase UAP56	5	62	10
Heat shock protein 90 alpha	9	111	15
Heat shock protein 90 beta	9	73	14
Heat shock cognate 71-kDa protein	11	134	15
Heat shock 70-kDa protein 1	12	120	14

intracellular localization of YB-1 in influenza virus-infected cells by indirect immunofluorescence assays using anti-YB-1 antibody (Fig. 1B). The vRNA was also counterstained by the fluorescence *in situ* hybridization (FISH) method (28). YB-1 localized at the cytoplasm in infected cells at 4 hpi, as it did in mock-infected cells. Along with the progression of infection, YB-1 was imported to the nucleus and accumulated in unknown nuclear speckles at 8 hpi. At 12 hpi, a portion of YB-1 was found in unknown cytoplasmic granules with the exported progeny vRNA. Since these cytoplasmic granules of YB-1 were not found in the presence of LMB, a potent inhibitor of CRM1, it is likely that YB-1 is exported with vRNA from the nucleus (Fig. 1B). Furthermore, the translocation of YB-1 upon influenza virus infection may not be involved in the innate immunity, since the localization of YB-1 was not changed in Sendai virus-infected cells (Fig. 1B). Next, we examined the intracellular localization of RAP55, RCK/p54, and TIAR proteins, which are components of cellular mRNP and accumulate in SGs and P-bodies (2). In contrast to the case for YB-1, we did not find any localization changes of these proteins in response to infection (Fig. 1C). Thus, the translocation of YB-1 found in infected cells may not be involved in a function as a component of SGs and P-bodies.

Interaction of YB-1 with vRNP-exporting complexes. Progeny vRNP is exported to the cytoplasm from the nucleus through the CRM1-dependent pathway by assembling export complexes with viral proteins M1 and NS2 (19, 52, 54, 77). Since YB-1 may be exported to the cytoplasm together with vRNP, it is assumed that YB-1 interacts with vRNP export complexes in the nucleus. To address this, we examined the colocalization of YB-1 with M1 and NS2. We found that M1 but not NS2 accumulated in the nuclear speckles with YB-1 at 8 hpi (Fig. 2A). Since a major portion of the progeny vRNA and NS2 was localized in the cytoplasm (Fig. 1B and 2A), the newly synthesized vRNP may be exported to the cytoplasm immediately after formation of the export complex. Thus, we examined the localization of vRNA and NS2 in LMB-

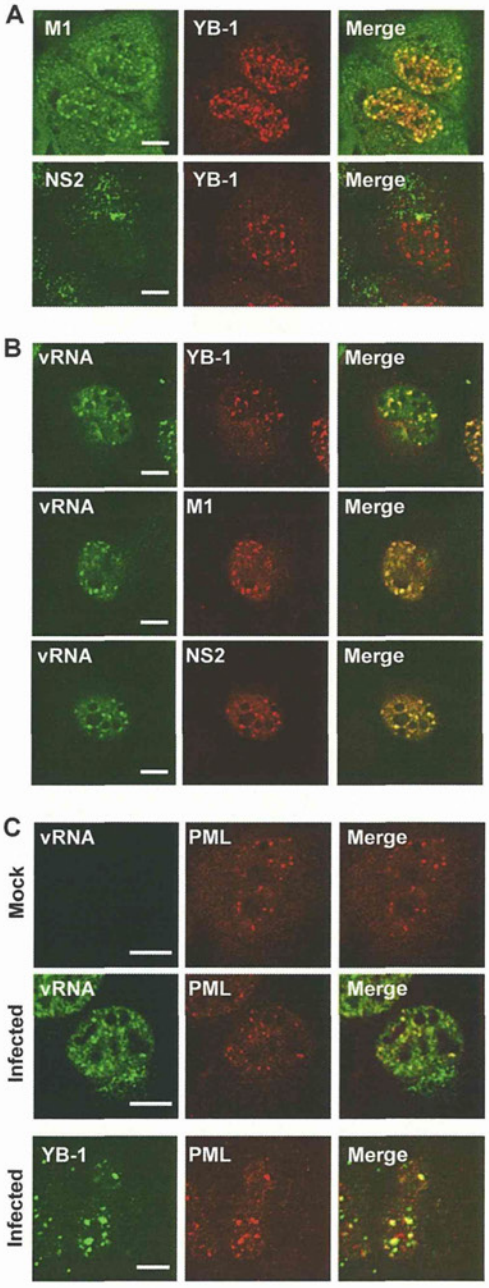

FIG 2 Colocalization of YB-1 and vRNP export complexes in nuclear speckles. (A) Intracellular localization of YB-1, M1, and NS2. At 8 hpi, infected MDCK cells were subjected to indirect immunofluorescence assays with rabbit anti-YB-1 (red) and either mouse anti-M1 (upper panel, green) or rat anti-NS2 (lower panel, green) antibody. Scale bar, 10 μm. (B) Intracellular localization of vRNA, YB-1, M1, and NS2 in the presence of LMB. At 7 hpi, infected MDCK cells were incubated for 1 h in the presence of 20 nM LMB. Segment 1 vRNA (left panels, green), YB-1 (upper panel, red), M1 (middle panel, red), and NS2 (lower panel, red) were visualized by FISH and indirect immunofluorescence assays. Scale bars, 10 μm. (C) Accumulation of vRNA and YB-1 in PML NBs in the presence of LMB. After treatment of LMB as described for panel B, mock-infected (upper panel) and infected (middle and lower panels) MDCK cells were subjected to FISH assays using the probe that hybridizes with segment 1 vRNA (upper and middle panels, green) and to indirect immunofluorescence assays with rabbit (upper and middle panels, red) and mouse (lower panel, red) anti-PML and rabbit anti-YB-1 antibodies (lower panel, green). Scale bars, 10 μm.

treated cells. Upon inhibition of the CRM1-dependent export pathway, vRNA accumulated in the nuclear speckles with YB-1, M1, and NS2 (Fig. 2B). Previously, it was reported that a small portion of M1 and NS2 may localize in PML NBs (62, 64). It has been shown that the overexpression of PML suppresses influenza virus proliferation (10, 27), suggesting that PML NBs may contribute to the cellular antiviral response. However, the role of PML NBs remains controversial, since influenza virus replicates normally in cells lacking the *PML* gene (20). As expected, in the presence of LMB, we found that vRNA and YB-1 were partially associated with PML NBs (Fig. 2C). Taking these findings together, it is possible that the YB-1 imported into the nucleus interacts with the vRNP export complexes in PML NBs and then YB-1 is subsequently exported from the nucleus with vRNP.

Influenza virus produces three different RNAs, i.e., vRNA, cRNA, and viral mRNA. Both vRNA and cRNA form ribonucleoprotein complexes with the viral polymerase and NP, whereas vRNA, but not cRNA, is found in the cytoplasm (26) and packaged into the virions. In contrast, the viral mRNA interacts with cellular mRNA-binding proteins and is exported through the REF/Aly pathway generally used by cellular mRNAs (4, 57). To examine the specific interaction of YB-1 with viral RNAs, we visualized positive-sense RNAs (cRNA and viral mRNA) by FISH assays. The intracellular localization of positive-sense RNAs was not changed by LMB treatment, as previously reported (57), and the FISH signals were not colocalized with YB-1 in the absence or presence of LMB (Fig. 3A). Further, to show quantitative results, we performed immunoprecipitation assays with cell lysates prepared from cells constitutively expressing FLAG-YB-1 using anti-FLAG antibody as described in Materials and Methods. We found that vRNA interacted with YB-1, but neither cRNA nor viral mRNA did in infected cells (Fig. 3B). Thus, it is quite likely that YB-1 is involved in the functional regulation of vRNP but not in that of either cRNP or viral mRNP.

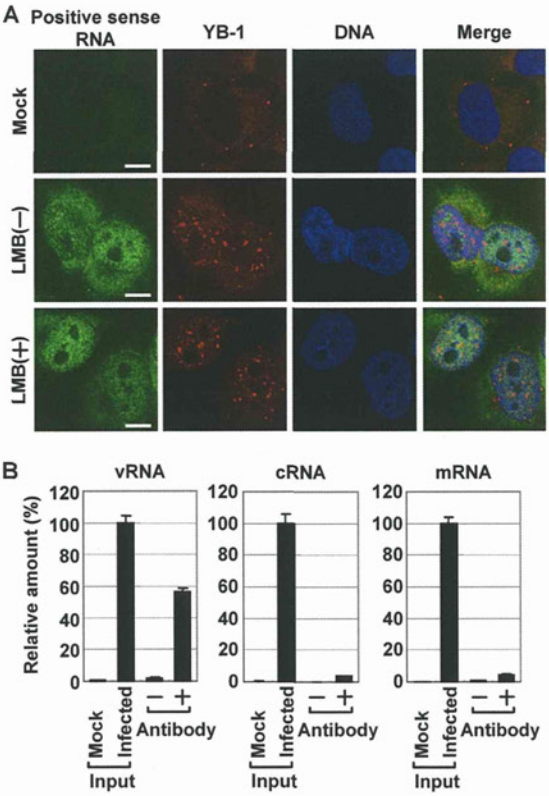

FIG 3 Specific interaction of YB-1 with vRNA but not with either cRNA or viral mRNA. (A) Intracellular localization of YB-1 and viral mRNA/cRNA. At 8 hpi, infected MDCK cells were subjected to FISH assays using a probe that hybridizes with segment 1 cRNA and mRNA (green) and to indirect immunofluorescence assays with anti-YB-1 antibody (red) with or without 20 nM LMB treatment for 1 h. Nuclear DNA was stained with TO-PRO-3 iodide (blue). Scale bars, 10 μm. (B) Coimmunoprecipitation of YB-1 and viral RNA molecules. HeLa cells constitutively expressing FLAG-YB-1 were infected with influenza virus at an MOI of 10. After 8 hpi, cell lysates were prepared and subjected to immunoprecipitation assays in the presence of either control IgG or anti-FLAG antibody as described in Materials and Methods. The immunoprecipitated viral RNAs were eluted with 100 μg/ml FLAG peptide and then quantitatively analyzed by reverse transcription followed by real-time PCR with primers specific for segment 5 vRNA, cRNA, and NP mRNA. To quantitatively evaluate the data, 5% equivalents of mock-infected and infected samples were also observed.

Interaction of the YB-1-vRNP complex with Rab11a-positive recycling endosomes along microtubules. At 12 hpi, YB-1 was partially colocalized with the vRNA exported from the nucleus in the cytoplasm (Fig. 1B). Recent studies have suggested that the progeny vRNP is transported to the plasma membrane along microtubules via Rab11a-positive recycling endosomes (1, 17, 47). Further, it has been reported that YB-1 interacts with microtubules (12). Based on these findings, we examined whether YB-1 accumulates in microtubules with vRNP (Fig. 4). We found that the cytoplasmic punctate signals of YB-1 in perinuclear regions were colocalized with α-tubulin (Fig. 4A). We then examined the interaction of YB-1 with microtubules, Rab11a, and vRNP by immunoprecipitation assays. YB-1 interacted with α-tubulin but hardly with Rab11a in mock-infected cells (Fig. 4B, lane 3). In contrast, the interaction of YB-1 with Rab11a was significantly increased in infected cells (Fig. 4B, lane 6). To address whether the vRNP-YB-1 complexes accumulate in microtubules with Rab11a, the proteins coprecipitated with YB-1 from infected lysates (Fig. 4B, lane 6) were eluted and then subjected to reimmunoprecipitation with anti-NP antibody (Fig. 4C). Since α-tubulin and Rab11a were immunoprecipitated with anti-NP antibody (Fig. 4C, lane 3), it is quite likely that the progeny vRNP is accumulated on Rab11a-positive recycling endosomes with YB-1 along microtubules.

YB-1 is a positive factor for Rab11a-dependent virus production. It has been shown that Rab11a is required for the transport of vRNP to the apical plasma membrane and thereby affects the production of progeny virions (1, 17, 47). Since YB-1 binds to Rab11a together with vRNP (Fig. 4C), it is assumed that YB-1 is involved in production of progeny virions through the Rab11a-positive recycling endosome pathway. To address this, the effect of YB-1 overexpression on the virus titer was examined using siRNA-mediated Rab11a knockdown (KD) cells (Fig. 5). The transfection efficiency was approximately 60%. The amount of exogenously overexpressed FLAG-YB-1 was 3-fold higher than that of endogenous YB-1, and the expression level of Rab11a in KD cells decreased to approximately 30% of that in control cells transfected with the nontargeting siRNA (Fig. 5A). The expression level of viral proteins was found to be virtually unchanged by YB-1 overexpression (Fig. 5B). We found that the amount of infectious virions produced from cells overexpressing YB-1 was significantly increased compared to that produced from cells transfected with empty plasmid, whereas the virus titer was slightly enhanced by

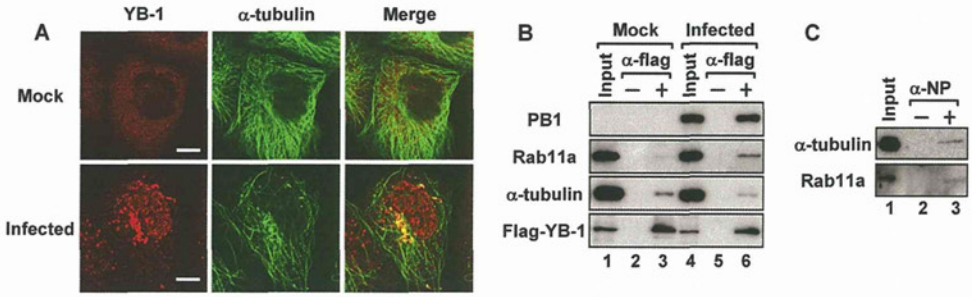

FIG 4 Accumulation of YB-1-vRNP complexes on microtubules with Rab11a-positive recycling endosomes in response to infection. (A) Colocalization of YB-1 and microtubules in cytoplasmic punctate signals. At 12 hpi, mock-infected (upper panels) and infected (lower panels) MDCK cells were subjected to indirect immunofluorescence assays with anti-YB-1 (red) and α-tubulin (green) antibodies. Scale bars, 10 μm. (B and C) Interaction of YB-1 with Rab11a-positive recycling endosomes on microtubules. HeLa cells constitutively expressing FLAG-YB-1 were infected with influenza virus at an MOI of 10. (B) Cell lysates were prepared and subjected to immunoprecipitation assays in the presence of either control IgG (lanes 2 and 5) or anti-FLAG antibody (lanes 3 and 6) at 12 hpi. Coprecipitated proteins were eluted with 100 μg/ml FLAG peptide and detected by Western blotting assays with anti-PB1, anti-Rab11a, anti-α-tubulin, and anti-FLAG antibodies. Ten percent equivalents of mock-infected (lane 1) and infected (lane 4) lysates were also subjected to Western blotting assays. (C) The eluate purified from infected lysate from panel B, lane 6, was reimmunoprecipitated with either control IgG (lane 2) or anti-NP antibody (lane 3), and then the eluate was subjected to Western blotting assays with anti-α-tubulin and anti-Rab11a antibodies. Lane 1, 30% equivalent of proteins immunopurified with anti-FLAG antibody from infected cell lysate.

YB-1 overexpression in Rab11a KD cells (Fig. 5C). Further, the slopes of the lines in Fig. 5C were determined to compare the efficiencies of virus production (Fig. 5D). This result shows that the production of infectious viruses was increased 4.8-fold by the YB-1 overexpression, but the stimulatory activity of YB-1 was reduced 1.9-fold by Rab11a KD (Fig. 5D). Therefore, it is concluded that YB-1 stimulates the production of infectious viruses in an Rab11a-dependent manner. We also tried to measure the amount of infectious virions produced from YB-1 KD cells. However, YB-1 KD cells tend to die from influenza virus infection after 16 to 20 hpi (data not shown). Thus, it was difficult to demonstrate the effect of YB-1 on the virus titer using YB-1 siRNA.

YB-1 functions as a porter for vRNP to direct it to microtubules. Figures 4 and 5 suggested that YB-1 functions in the vRNP transport through the Rab11a-positive recycling endosome pathway along microtubules. Next, we tried to demonstrate whether YB-1 functions as a transporter of vRNP to microtubules using siRNA-mediated gene silencing (Fig. 6). At 48 h after transfection of YB-1 siRNA, the expression level of YB-1 in KD cells decreased to 25% of that in control cells (Fig. 6A). There were no differences found in the accumulation levels of viral proteins (Fig. 6B) and vRNA and viral mRNA (Fig. 6C) between control and YB-1 KD cells. Previous reports showed that the vRNP complexes exported from the nucleus accumulate at the MTOC around the perinucleus (45) with Rab11a-positive recycling endosomes (1, 17, 47). We carried out FISH assays to examine whether vRNP complexes localize around the perinucleus in YB-1 KD cells at 8 hpi (Fig. 6D and E). A major population of YB-1 KD cells (81.5% ± 7.2%) had vRNA in a diffusive pattern. Thus, it is quite likely that YB-1 stimulates the accumulation of vRNP at the MTOC. As shown in Fig. 2C, the replicated vRNA associated with PML NBs in the presence of LMB. Since vRNA accumulated in PML NBs even in YB-1 KD cells with LMB treatment (Fig. 6D), it is strongly suggested that YB-1 is not involved in the association between vRNP and PML NBs. It is reported that exogenously expressed M1 is localized in PML NBs (64), suggesting that vRNP might accumulate in PML NBs through the interaction between vRNP and M1. It is also suggested that YB-1 does not play a role in the vRNP export from the nucleus to the cytoplasm, since vRNA was found predominantly in the cytoplasm of YB-1 KD cells (Fig. 6E).

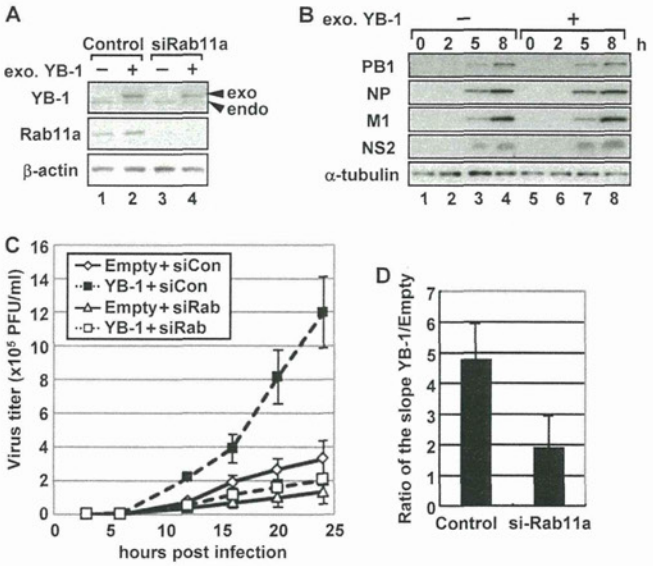

FIG 5 Effect of YB-1 overexpression on the production of infectious virions. (A) Expression levels of YB-1 and Rab11a proteins. 293T cells were transfected with either pCAGGS empty plasmid (lanes 1 and 3) or pCAGGS-FLAG-YB-1 (lanes 2 and 4) at 24 h after treatment of either nontargeting (control; lanes 1 and 2) or Rab11a (siRab11a; lanes 3 and 4) siRNA. At 24 h after transfection of expression vectors, the cell lysates were prepared and analyzed by SDS-PAGE followed by Western blotting assays with anti-YB-1, anti-Rab11a, and anti-β-actin antibodies. (B) Accumulation levels of viral proteins in cells overexpressing FLAG-YB-1. 293T cells were transfected with either pCAGGS or pCAGGS-FLAG-YB-1. At 24 h posttransfection, cells were infected with influenza virus at an MOI of 10. At 0, 2, 5, and 8 hpi, cell lysates were prepared and analyzed by Western blotting assays with anti-PB1, anti-NP, anti-M1, anti-NS2, and anti-α-tubulin antibodies. (C) Production of infectious virions. Control (open diamonds and filled squares) and Rab11a KD 293T (open triangles and open squares) cells transfected with either pCAGGS (open diamonds and open triangles) or pCAGGS-FLAG-YB-1 (filled and open squares) as described for panel A were infected with influenza virus at an MOI of 0.5. The culture supernatants collected at 3, 6, 12, 16, 20, and 24 hpi were subjected to plaque assays to examine the production of infectious virions in a single-round infection. The average titers and standard deviations determined from three independent experiments are shown. (D) Stimulatory activity of YB-1 on the virus titer in Rab11a KD cells. The slopes of the lines in panel C were determined by the least-squares method, and the ratio of the virus titer from cells overexpressing FLAG-YB-1 to that from cells transfected with pCAGGS is shown.

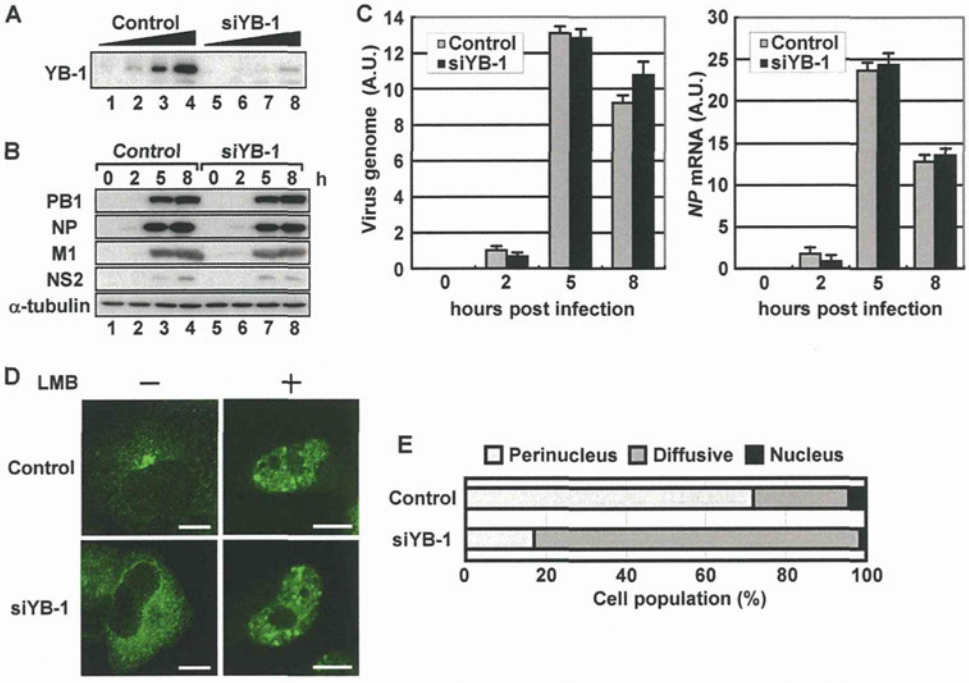

FIG 6 Accumulation of vRNP on microtubules in YB-1 knockdown cells. (A) Expression level of YB-1 in YB-1 KD cells. HeLa cells transfected with nontargeting (control; lanes 1 to 4) or YB-1 (siYB-1; lanes 5 to 8) siRNA were lysed, and then the lysates (2.5×10^3, 5×10^3, 1×10^4, and 2×10^4 cells) were subjected to SDS-PAGE followed by Western blotting assays with anti-YB-1 antibody at 48 h posttransfection. (B and C) Accumulation levels of viral proteins and RNAs in YB-1 KD cells. At 48 posttransfection of siRNA, control and YB-1 KD cells were infected with influenza virus at an MOI of 10. At 0, 2, 5, and 8 hpi, cell lysates were prepared and analyzed by Western blotting assays with anti-PB1, anti-NP, anti-M1, anti-NS2, and anti-α-tubulin antibodies. Total RNAs purified from the cells at 0, 2, 5, and 8 hpi were subjected to reverse transcription followed by quantitative real-time PCR with primers specific for segment 5 vRNA and NP mRNA as described in Materials and Methods. (D and E) Intracellular localization of vRNA in YB-1 KD cells. At 8 hpi with or without LMB treatment for 1 h, infected control and YB-1 KD cells were subjected to FISH assays using a probe that hybridizes with segment 1 vRNA (panel D) (scale bars, 10 μm). Cells were counted, and the localization pattern of vRNA in the absence of LMB was determined (E). The number of cells showing each localization pattern was expressed as the percentage of the total cell number ($n = 80$) in panel E. The average percentages determined from three independent experiments are shown.

YB-1 interacts with vRNP (Fig. 1A and 4B), but it is unclear whether YB-1 interacts directly with one or more vRNP components, that is, viral polymerase complexes, NP, and vRNA. To test this, we performed pulldown assays with purified vRNP and His-YB-1 using Ni-nitrilotriacetic acid (NTA) resin (Fig. 7A). Not only viral polymerase subunits but also NP was coprecipitated with YB-1 (lane 6), demonstrating that YB-1 interacts directly with vRNP. Since YB-1 has a single-stranded RNA binding activity, it is possible that YB-1 binds to vRNA. To address this, vRNP treated with micrococcal nuclease (mnRNP) to deplete vRNA was also subjected to the pulldown assay with His-YB-1. We found that each viral polymerase subunit but not NP from mnRNP was coprecipitated with YB-1 (Fig. 7A, lane 9), suggesting that YB-1 interacts with viral polymerase complexes. YB-1 consists of three domains: the N-terminal domain, the cold shock domain (CSD), and the C-terminal tail domain. The CSD has the well-characterized RNA-binding motifs RNP-1 and RNP-2 and thereby functions as a nucleic acid-binding domain. The N-terminal domain is rich in alanine and proline (A/P domain), and the C-terminal domain contains alternating clusters of positively and negatively charged amino acid residues (A/B domain). All three domains are involved in interaction with a number of cellular proteins (reviewed in reference 18). To further characterize the interaction between YB-1 and vRNP, we carried out pulldown assays with GST-fused deletion mutants of YB-1 and vRNP (Fig, 7B). We found that PB1 is coprecipitated with the mutants harboring the A/B domain (lanes 5 and 6; ΔA/P and A/B), suggesting that YB-1 interacts with vRNP through the A/B domain. Next, we tried to demonstrate whether YB-1 recruits vRNP on microtubules *in vitro*. Reconstituted microtubules were incubated with either vRNP or YB-1-vRNP complex and then subjected to immunoprecipitation using anti-NP antibody (Fig. 7C). We found that microtubules were hardly coprecipitated with vRNP in the absence of YB-1 (lane 4). In sharp contrast, in the presence of YB-1, the interaction of vRNP with microtubules was increased by approximately 3-fold (lane 5). Finally, we carried out immunoprecipitation assays with cell lysates prepared from cells constitutively expressing FLAG-α-tubulin with or without YB-1 KD (Fig. 7D). We found that PB1 was immunoprecipitated with FLAG-α-tubulin from control lysates (lane 3) but slightly from YB-1 KD lysates (lane 6). Therefore, it could be concluded that YB-1 is required for the accumulation of vRNP on microtubules. Taking these findings together, we propose that YB-1 interacts directly with vRNP and functions as a porter that facilitates the binding of vRNP with microtubules, where vRNP is led to Rab11a-positivie recycling endosomes.

DISCUSSION

We have identified YB-1, a cellular DNA/RNA-binding protein, as a vRNP-interacting protein (Fig. 1A). YB-1 was found to be relocalized to the nucleus from the cytoplasm and associated with PML NBs along with the progression of virus infection (Fig. 1B).

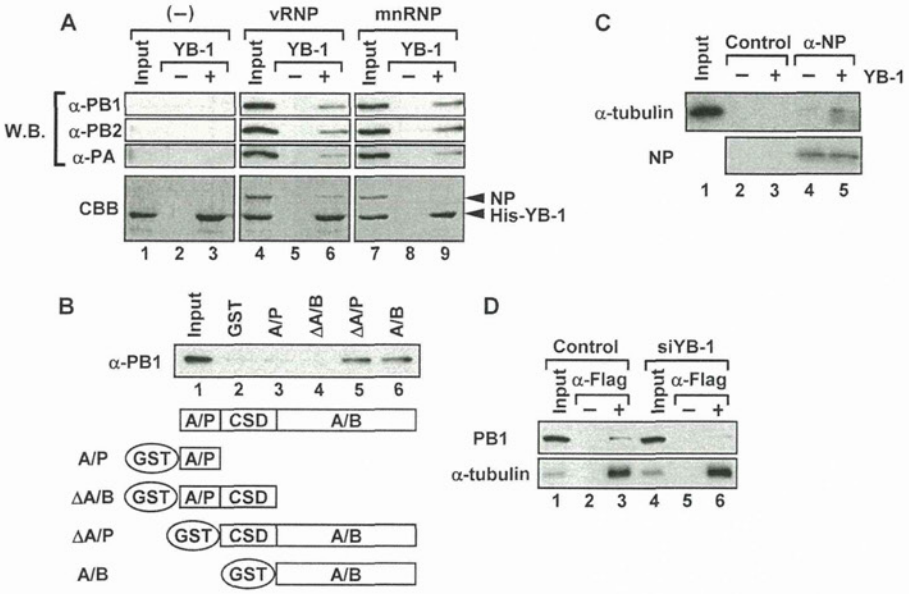

FIG 7 YB-1 functions as a porter bringing the progeny vRNP to microtubules. (A) Direct interaction of YB-1 with viral polymerase complex. vRNP (lanes 4 to 6) or micrococcal nuclease-treated vRNP (mnRNP) (lanes 7 to 9) was incubated in the absence (lanes 2, 5, and 8) or presence (lanes 3, 6, and 9) of purified recombinant His-YB-1 protein at 30°C for 1 h. Complexes were purified using Ni-NTA resin, and then proteins were separated through SDS-PAGE and detected by Coomassie brilliant blue (CBB) staining and Western blotting assays with anti-PB1, anti-PB2, and anti-PA antibodies. Lanes 1, 4, and 7 represent 20% of input amounts. (B) Interaction of vRNP with deletion mutants of YB-1. Each GST-fused deletion mutant of YB-1 was incubated with vRNP at 30°C for 1 h. Complexes were purified using glutathione-Sepharose resins, and then proteins were separated through SDS-PAGE and detected by Western blotting assays using anti-PB1 antibody. Lane 1 represents 20% of input amounts. A schematic diagram of the deletion mutants of YB-1 is at the bottom. (C) Interaction between vRNP and microtubules mediated by YB-1. Reconstituted microtubules were incubated with either vRNP (lanes 2 and 4) or YB-1-vRNP complex (lanes 3 and 5), and then complexes were immunoprecipitated with either a nonspecific IgG (control; lanes 2 and 3) or anti-NP antibody (lanes 4 and 5). The immunoprecipitated proteins were separated through SDS-PAGE and subjected to Western blotting assays with anti-α-tubulin and anti-NP antibodies. Lane 1 represents 10% of input amount. (D) Interaction of vRNP with microtubules in YB-1 KD cells. HeLa cells constitutively expressing FLAG-α-tubulin were infected with influenza virus at an MOI of 10. At 8 hpi, cell lysates were prepared and subjected to immunoprecipitation assays with either control IgG or anti-FLAG antibody. The immunoprecipitated proteins eluted with 100 μg/ml FLAG peptide were separated through SDS-PAGE and then visualized by Western blotting assays using anti-PB1 and anti-α-tubulin antibodies. Five percent equivalents of control (lane 1) and YB-1 KD (lane 4) lysates are also shown.

Previous reports showed that the nuclear import of YB-1 requires phosphorylation by protein kinase C (PKC) (35) and Jak1 (15) and Akt (69) kinases. The other mechanism for nuclear import of YB-1 is thought to be triggered by a proteolytic cleavage by 20S proteasomes to separate the C-terminal fragment (aa 220 to 324) containing a cytoplasmic retention signal (68). When we performed immunofluorescence assays with an antibody recognizing either the N terminus (aa 1 to 13) (used in this study) or the C terminus (aa 307 to 324) (purchased from Sigma), the YB-1 nuclear import was found only when the antibody recognizing the N terminus was used (data not shown). However, we found that vRNP complexes interact with full-length YB-1 (Fig. 1A), suggesting that the 20S proteasome-mediated processing of YB-1 may not always be required in influenza virus-infected cells. Therefore, it is possible that the recognition specificity of our antibody is due to an unknown conformational change of YB-1 possibly induced by the phosphorylation and/or interaction with cellular and/or viral proteins. Identification of a signaling pathway and interacting proteins responsible for the nuclear import of YB-1 upon influenza virus infection is needed.

PML NBs are highly dynamic structures that are disrupted or changed in their morphology in response to environmental stimuli (38). The genomes of several DNA viruses have been shown to be localized and transcribed in the vicinity of PML NBs (13, 23, 24). In most cases, virus-encoded regulatory proteins localize at PML NBs and disrupt PML NBs for successful infection, suggesting a negative role for PML NBs in virus growth (13, 23, 24). In addition to the putative function of PML NBs during virus infection, it is postulated that PML NBs have functions in cellular gene transcription, tumor suppression, proteasomal degradation, cellular senescence, apoptosis, and DNA repair (14, 38). It is proposed that PML NBs might modulate chromatin architecture and transcription, since nascent RNA and several gene loci are found around PML NBs (5, 13, 65). Given this, it seems likely that viruses hijack this nuclear structure to set up a platform suitable for virus replication, although the functional relevance of the interaction between influenza virus and PML NBs is an open question. M1 and NS2 were shown to be associated with PML NBs (62, 64), although the functional significance of the colocalization remains to be determined. We found that the YB-1 imported into the nucleus accumulates in PML NBs, in which vRNA was present with M1 and NS2 when the vRNP export was inhibited (Fig. 2). Therefore, we speculate that the progeny vRNPs could be assembled into the export complexes at PML NBs and subsequently interact with YB-1. Additional experiments are needed to clarify a precise role(s) of PML NBs in the vRNP nuclear export as well as the mechanism for targeting YB-1 to PML NBs.

The accumulation of recycling endosome vesicles around the MTOC is disrupted in the presence of microtubule depolymerization reagents such as nocodazole (8). Thus, it is likely that the intact microtubule functions as a platform for the recycling endosome vesicle. We observed a direct binding of YB-1 with vRNP for

the recruitment of vRNP to microtubules (Fig. 7). However, only a small portion of vRNP was colocalized with YB-1 in infected cells, suggesting that YB-1 transiently interacts with vRNP (Fig. 1). Further, we could not find YB-1 in the purified influenza virions (data not shown), suggesting that YB-1 might be dissociated from vRNP prior to packaging of vRNP into progeny virions. The association between YB-1 and enough microtubules is proposed to compete with the interaction of YB-1 with cellular mRNP *in vitro* (11). Thus, we speculate that vRNP-YB-1 complexes recruited on microtubules may be disassembled by the microtubule formation, and thereby vRNP could be loaded onto Rab11a-positive recycling endosomes bound to microtubules.

The Rab11a-mediated vesicular transport may be functionally important after arrival at the plasma membrane. For example, lipid rafts are required for the budding of influenza virus from the apical plasma membrane (63, 70), and cholesterol, an essential component of the lipid rafts, is enriched in the recycling endosome membrane (48). Interestingly, it has been shown that influenza virus particles are hardly pinched off from the plasma membrane in Rab11a KD cells (7). Thus, it is possible that the Rab11a-positive recycling endosome has an important role in the apical transport of proteins and/or membranes which are involved in budding process, including membrane scission (60). However, it is also possible that the trafficking of the viral genome is required to allow the efficient virus budding. The influenza virus genome consists of eight-segmented vRNA molecules. Since it is believed that the eight individual segments are packaged into a progeny virion (53), a hierarchical incorporation of each vRNA should be required. It is hypothesized that Rab11a-positive transport vesicles might be an assembly center of the eight segments of vRNA (17, 47). To further understand the mechanism of influenza virus egress, the dynamics of the recycling endocytic compartment are to be analyzed.

ACKNOWLEDGMENTS

We thank F. Momose (Kitasato University) for helpful discussion and K. Mizumoto (Kitasato University), K. Irie (University of Tsukuba), T. Naiki (University of Tsukuba), A. Kato (National Institute of Infectious Diseases, Japan), S. Hongo (Yamagata University), and K. Sugawara (Yamagata University) for generous gifts of purified tubulin proteins (K. Mizumoto), anti-TIAR antibody (K. Irie and T. Naiki), anti-SeV antibody (A. Kato), and mouse monoclonal anti-M1 antibody (S. Hongo and K. Sugawara). We also thank M. N. Asaka (University of Tsukuba) and T. Minowa (National Institute for Material Science) for their help with LC-MS analysis.

This research was supported in part by a grant-in-aid from the Ministry of Education, Culture, Sports, Science, and Technology of Japan (to K.N.) and Research Fellowships of the Japanese Society for the Promotion of Science (JSPS) (to A.K.).

REFERENCES

1. **Amorim MJ, et al.** 2011. A Rab11- and microtubule-dependent mechanism for cytoplasmic transport of influenza A virus viral RNA. J. Virol. **85**:4143–4156.
2. **Anderson P, Kedersha N.** 2008. Stress granules: the Tao of RNA triage. Trends Biochem. Sci. **33**:141–150.
3. **Anderson P, Kedersha N.** 2002. Stressful initiations. J. Cell Sci. **115**:3227–3234.
4. **Bier K, York A, Fodor E.** 2011. Cellular cap-binding proteins associate with influenza virus mRNAs. J. Gen. Virol. **92**:1627–1634.
5. **Boisvert FM, Hendzel MJ, Bazett-Jones DP.** 2000. Promyelocytic leukemia (PML) nuclear bodies are protein structures that do not accumulate RNA. J. Cell Biol. **148**:283–292.
6. **Brock SC, Goldenring Jr, Crowe JE, Jr.** 2003. Apical recycling systems regulate directional budding of respiratory syncytial virus from polarized epithelial cells. Proc. Natl. Acad. Sci. U. S. A. **100**:15143–15148.
7. **Bruce EA, Digard P, Stuart AD.** 2010. The Rab11 pathway is required for influenza A virus budding and filament formation. J. Virol. **84**:5848–5859.
8. **Casanova JE, et al.** 1999. Association of Rab25 and Rab11a with the apical recycling system of polarized Madin-Darby canine kidney cells. Mol. Biol. Cell **10**:47–61.
9. **Chambers R, Takimoto T.** 2010. Trafficking of Sendai virus nucleocapsids is mediated by intracellular vesicles. PLoS One **5**:e10994. doi:10.1371/journal.pone.0010994.
10. **Chelbi-Alix MK, Quignon F, Pelicano L, Koken MH, de The H.** 1998. Resistance to virus infection conferred by the interferon-induced promyelocytic leukemia protein. J. Virol. **72**:1043–1051.
11. **Chernov KG, et al.** 2008. Atomic force microscopy reveals binding of mRNA to microtubules mediated by two major mRNP proteins YB-1 and PABP. FEBS Lett. **582**:2875–2881.
12. **Chernov KG, et al.** 2008. YB-1 promotes microtubule assembly in vitro through interaction with tubulin and microtubules. BMC Biochem. **9**:23. doi:10.1186/1471-2091-9-23.
13. **Ching RW, Dellaire G, Eskiw CH, Bazett-Jones DP.** 2005. PML bodies: a meeting place for genomic loci? J. Cell Sci. **118**:847–854.
14. **Dellaire G, Bazett-Jones DP.** 2004. PML nuclear bodies: dynamic sensors of DNA damage and cellular stress. Bioessays **26**:963–977.
15. **Dooley S, et al.** 2006. Y-box protein-1 is the crucial mediator of antifibrotic interferon-gamma effects. J. Biol. Chem. **281**:1784–1795.
16. **Dreyfuss G, Kim VN, Kataoka N.** 2002. Messenger-RNA-binding proteins and the messages they carry. Nat. Rev. Mol. Cell Biol. **3**:195–205.
17. **Eisfeld AJ, Kawakami E, Watanabe T, Neumann G, Kawaoka Y.** 2011. RAB11A is essential for transport of the influenza virus genome to the plasma membrane. J. Virol. **85**:6117–6126.
18. **Eliseeva IA, Kim ER, Guryanov SG, Ovchinnikov LP, Lyabin DN.** 2011. Y-box-binding protein 1 (YB-1) and its functions. Biochemistry (Mosc.) **76**:1402–1433.
19. **Elton D, et al.** 2001. Interaction of the influenza virus nucleoprotein with the cellular CRM1-mediated nuclear export pathway. J. Virol. **75**:408–419.
20. **Engelhardt OG, Sirma H, Pandolfi PP, Haller O.** 2004. Mx1 GTPase accumulates in distinct nuclear domains and inhibits influenza A virus in cells that lack promyelocytic leukaemia protein nuclear bodies. J. Gen. Virol. **85**:2315–2326.
21. **Eulalio A, Behm-Ansmant I, Izaurralde E.** 2007. P bodies: at the crossroads of post-transcriptional pathways. Nat. Rev. Mol. Cell Biol. **8**:9–22.
22. **Evdokimova V, et al.** 2001. The major mRNA-associated protein YB-1 is a potent 5′ cap-dependent mRNA stabilizer. EMBO J. **20**:5491–5502.
23. **Everett RD.** 2006. Interactions between DNA viruses, ND10 and the DNA damage response. Cell. Microbiol. **8**:365–374.
24. **Everett RD, Chelbi-Alix MK.** 2007. PML and PML nuclear bodies: implications in antiviral defence. Biochimie **89**:819–830.
25. **Grant BD, Donaldson JG.** 2009. Pathways and mechanisms of endocytic recycling. Nat. Rev. Mol. Cell Biol. **10**:597–608.
26. **Herz C, Stavnezer E, Krug R, Gurney T.** 1981. Influenza virus, an RNA virus, synthesizes its messenger RNA in the nucleus of infected cells. Cell **26**:391–400.
27. **Iki S, et al.** 2005. Serum-dependent expression of promyelocytic leukemia protein suppresses propagation of influenza virus. Virology **343**:106–115.
28. **Jo S, et al.** 2010. Involvement of vesicular trafficking system in membrane targeting of the progeny influenza virus genome. Microbes Infect. **12**:1079–1084.
29. **Jorba N, et al.** 2008. Analysis of the interaction of influenza virus polymerase complex with human cell factors. Proteomics **8**:2077–2088.
30. **Kawaguchi A, Momose F, Nagata K.** 2011. Replication-coupled and host factor-mediated encapsidation of the influenza virus genome by viral nucleoprotein. J. Virol. **85**:6197–6204.
31. **Kawaguchi A, Naito T, Nagata K.** 2005. Involvement of influenza virus PA subunit in assembly of functional RNA polymerase complexes. J. Virol. **79**:732–744.
32. **Kawakami K, Ishihama A.** 1983. RNA polymerase of influenza virus. III. Isolation of RNA polymerase-RNA complexes from influenza virus PR8. J. Biochem. **93**:989–996.

33. **Keene JD.** 2010. Global regulation and dynamics of ribonucleic acid. Endocrinology **151**:1391–1397.
34. **Kohno K, Izumi H, Uchiumi T, Ashizuka M, Kuwano M.** 2003. The pleiotropic functions of the Y-box-binding protein, YB-1. Bioessays **25**: 691–698.
35. **Koike K, et al.** 1997. Nuclear translocation of the Y-box binding protein by ultraviolet irradiation. FEBS Lett. **417**:390–394.
36. **Krzyzaniak MA, Mach M, Britt WJ.** 2009. HCMV-encoded glycoprotein M (UL100) interacts with Rab11 effector protein FIP4. Traffic **10**:1439–1457.
37. **Kuwano M, et al.** 2003. The basic and clinical implications of ABC transporters, Y-box-binding protein-1 (YB-1) and angiogenesis-related factors in human malignancies. Cancer Sci. **94**:9–14.
38. **Lallemand-Breitenbach V, de The H.** 2010. PML nuclear bodies. Cold Spring Harbor Perspect. Biol. **2**:a000661. doi:10.1101/cshperspect.a000661.
39. **Martin K, Helenius A.** 1991. Nuclear transport of influenza virus ribonucleoproteins: the viral matrix protein (M1) promotes export and inhibits import. Cell **67**:117–130.
40. **Matsumoto K, et al.** PRMT1 is required for RAP55 to localize to processing bodies. RNA Biol. **9**:610–623.
41. **Matsumoto K, Wolffe AP.** 1998. Gene regulation by Y-box proteins: coupling control of transcription and translation. Trends Cell Biol. **8**:318–323.
42. **Maxfield FR, McGraw TE.** 2004. Endocytic recycling. Nat. Rev. Mol. Cell Biol. **5**:121–132.
43. **Mayer D, et al.** 2007. Identification of cellular interaction partners of the influenza virus ribonucleoprotein complex and polymerase complex using proteomic-based approaches. J. Proteome Res. **6**:672–682.
44. **Momose F, et al.** 2001. Cellular splicing factor RAF-2p48/NPI-5/BAT1/UAP56 interacts with the influenza virus nucleoprotein and enhances viral RNA synthesis. J. Virol. **75**:1899–1908.
45. **Momose F, Kikuchi Y, Komase K, Morikawa Y.** 2007. Visualization of microtubule-mediated transport of influenza viral progeny ribonucleoprotein. Microbes Infect. **9**:1422–1433.
46. **Momose F, et al.** 2002. Identification of Hsp90 as a stimulatory host factor involved in influenza virus RNA synthesis. J. Biol. Chem. **277**:45306–45314.
47. **Momose F, et al.** 2011. Apical transport of influenza A virus ribonucleoprotein requires Rab11-positive recycling endosome. PLoS One **6**:e21123. doi:10.1371/journal.pone.0021123.
48. **Mukherjee S, Zha X, Tabas I, Maxfield FR.** 1998. Cholesterol distribution in living cells: fluorescence imaging using dehydroergosterol as a fluorescent cholesterol analog. Biophys. J. **75**:1915–1925.
49. **Nagata K, Kawaguchi A, Naito T.** 2008. Host factors for replication and transcription of the influenza virus genome. Rev. Med. Virol. **18**:247–260.
50. **Naito T, Momose F, Kawaguchi A, Nagata K.** 2007. Involvement of Hsp90 in assembly and nuclear import of influenza virus RNA polymerase subunits. J. Virol. **81**:1339–1349.
51. **Nayak DP, Hui EK, Barman S.** 2004. Assembly and budding of influenza virus. Virus Res. **106**:147–165.
52. **Neumann G, Hughes MT, Kawaoka Y.** 2000. Influenza A virus NS2 protein mediates vRNP nuclear export through NES-independent interaction with hCRM1. EMBO J. **19**:6751–6758.
53. **Noda T, et al.** 2006. Architecture of ribonucleoprotein complexes in influenza A virus particles. Nature **439**:490–492.
54. **O'Neill RE, Talon J, Palese P.** 1998. The influenza virus NEP (NS2 protein) mediates the nuclear export of viral ribonucleoproteins. EMBO J. **17**:288–296.
55. **Pisarev AV, et al.** 2002. Positive and negative effects of the major mammalian messenger ribonucleoprotein p50 on binding of 40 S ribosomal subunits to the initiation codon of beta-globin mRNA. J. Biol. Chem. **277**:15445–15451.
56. **Portela A, Digard P.** 2002. The influenza virus nucleoprotein: a multifunctional RNA-binding protein pivotal to virus replication. J. Gen. Virol. **83**:723–734.
57. **Read EK, Digard P.** 2010. Individual influenza A virus mRNAs show differential dependence on cellular NXF1/TAP for their nuclear export. J. Gen. Virol. **91**:1290–1301.
58. **Rees PJ, Dimmock NJ.** 1981. Electrophoretic separation of influenza virus ribonucleoproteins. J. Gen. Virol. **53**:125–132.
59. **Robb NC, et al.** 2011. The influenza A virus NS1 protein interacts with the nucleoprotein of viral ribonucleoprotein complexes. J. Virol. **85**:5228–5231.
60. **Rossman JS, Jing X, Leser GP, Lamb RA.** 2010. Influenza virus M2 protein mediates ESCRT-independent membrane scission. Cell **142**:902–913.
61. **Rowe RK, Suszko JW, Pekosz A.** 2008. Roles for the recycling endosome, Rab8, and Rab11 in hantavirus release from epithelial cells. Virology **382**: 239–249.
62. **Sato Y, et al.** 2003. Localization of influenza virus proteins to nuclear dot 10 structures in influenza virus-infected cells. Virology **310**:29–40.
63. **Scheiffele P, Rietveld A, Wilk T, Simons K.** 1999. Influenza viruses select ordered lipid domains during budding from the plasma membrane. J. Biol. Chem. **274**:2038–2044.
64. **Shibata T, Tanaka T, Shimizu K, Hayakawa S, Kuroda K.** 2009. Immunofluorescence imaging of the influenza virus M1 protein is dependent on the fixation method. J. Virol. Methods **156**:162–165.
65. **Shiels C, et al.** 2001. PML bodies associate specifically with the MHC gene cluster in interphase nuclei. J. Cell Sci. **114**:3705–3716.
66. **Shimizu K, Handa H, Nakada S, Nagata K.** 1994. Regulation of influenza virus RNA polymerase activity by cellular and viral factors. Nucleic Acids Res. **22**:5047–5053.
67. **Sloboda RD, Dentler WL, Rosenbaum JL.** 1976. Microtubule-associated proteins and the stimulation of tubulin assembly in vitro. Biochemistry **15**:4497–4505.
68. **Sorokin AV, et al.** 2005. Proteasome-mediated cleavage of the Y-box-binding protein 1 is linked to DNA-damage stress response. EMBO J. **24**:3602–3612.
69. **Sutherland BW, et al.** 2005. Akt phosphorylates the Y-box binding protein 1 at Ser102 located in the cold shock domain and affects the anchorage-independent growth of breast cancer cells. Oncogene **24**:4281–4292.
70. **Takeda M, Leser GP, Russell CJ, Lamb RA.** 2003. Influenza virus hemagglutinin concentrates in lipid raft microdomains for efficient viral fusion. Proc. Natl. Acad. Sci. U. S. A. **100**:14610–14617.
71. **Tanaka KJ, et al.** 2006. RAP55, a cytoplasmic mRNP component, represses translation in Xenopus oocytes. J. Biol. Chem. **281**:40096–40106.
72. **Tay WL, et al.** 2009. Y-Box-binding protein-1 is a promising predictive marker of radioresistance and chemoradioresistance in nasopharyngeal cancer. Mod. Pathol. **22**:282–290.
73. **Utley TJ, et al.** 2008. Respiratory syncytial virus uses a Vps4-independent budding mechanism controlled by Rab11-FIP2. Proc. Natl. Acad. Sci. U. S. A. **105**:10209–10214.
74. **van Ijzendoorn SC.** 2006. Recycling endosomes. J. Cell Sci. **119**:1679–1681.
75. **Wakabayashi Y, Dutt P, Lippincott-Schwartz J, Arias IM.** 2005. Rab11a and myosin Vb are required for bile canalicular formation in WIF-B9 cells. Proc. Natl. Acad. Sci. U. S. A. **102**:15087–15092.
76. **Watanabe K, et al.** 2006. Identification of Hsc70 as an influenza virus matrix protein (M1) binding factor involved in the virus life cycle. FEBS Lett. **580**:5785–5790.
77. **Watanabe K, et al.** 2001. Inhibition of nuclear export of ribonucleoprotein complexes of influenza virus by leptomycin B. Virus Res. **77**:31–42.
78. **Yang WH, Bloch DB.** 2007. Probing the mRNA processing body using protein macroarrays and "autoantigenomics." RNA **13**:704–712.
79. **Zhang J, Pekosz A, Lamb RA.** 2000. Influenza virus assembly and lipid raft microdomains: a role for the cytoplasmic tails of the spike glycoproteins. J. Virol. **74**:4634–4644.

JVI
Journals.ASM.org

Replication-Uncoupled Histone Deposition during Adenovirus DNA Replication

Tetsuro Komatsu and Kyosuke Nagata

Department of Infection Biology, Faculty of Medicine and Graduate School of Comprehensive Human Sciences, University of Tsukuba, Tsukuba, Japan

In infected cells, the chromatin structure of the adenovirus genome DNA plays critical roles in its genome functions. Previously, we reported that in early phases of infection, incoming viral DNA is associated with both viral core protein VII and cellular histones. Here we show that in late phases of infection, newly synthesized viral DNA is also associated with histones. We also found that the knockdown of CAF-1, a histone chaperone that functions in the replication-coupled deposition of histones, does not affect the level of histone H3 bound on viral chromatin, although CAF-1 is accumulated at viral DNA replication foci together with PCNA. Chromatin immunoprecipitation assays using epitope-tagged histone H3 demonstrated that histone variant H3.3, which is deposited onto the cellular genome in a replication-independent manner, is selectively associated with both incoming and newly synthesized viral DNAs. Microscopic analyses indicated that histones but not USF1, a transcription factor that regulates viral late gene expression, are excluded from viral DNA replication foci and that this is achieved by the oligomerization of the DNA binding protein (DBP). Taken together, these results suggest that histone deposition onto newly synthesized viral DNA is most likely uncoupled with viral DNA replication, and a possible role of DBP oligomerization in this replication-uncoupled histone deposition is discussed.

In the cell nucleus, the genomic DNA is not naked but forms a chromatin structure with chromatin proteins. The fundamental unit of the chromatin structure is the nucleosome, which consists of a histone octamer (two copies each of histones H2A, H2B, H3, and H4) and DNA wrapping around the octamer. The deposition of histones and/or the remodeling of nucleosome arrays is a critical process for the expression of genome functions (2), since nucleosome packaging could be a barrier for *trans*-acting factors to access their cognate sites on DNA. Thus, the nucleosome structure must be strictly and dynamically regulated in connection with several events on chromatin, such as transcription, DNA replication, and DNA repair.

Currently, it is known that histone deposition is carried out mainly in two fashions, DNA replication-dependent and independent ones, and a role of histone variants in these deposition pathways has been elucidated (14). In mammalian somatic cells, there are three major histone H3 variants, H3.1, H3.2, and H3.3, and they have only slight differences in amino acid sequences (16). The canonical histone H3, histone H3.1, and the highly related variant H3.2 (which differs by only 1 amino acid [aa] from H3.1) are expressed exclusively during the S phase, while the expression of the variant H3.3, which differs by 4 and 5 aa from H3.2 and H3.1, respectively, is observed throughout the cell cycle. Thus, this variant is called a "replication-independent" one (11). Tagami et al. demonstrated previously that the canonical histone H3 (H3.1) interacts with the histone chaperone CAF-1 complex and is deposited onto DNA in a replication-dependent manner, while HIRA specifically binds to and deposits histone variant H3.3 onto DNA independently of DNA synthesis (43). CAF-1 is composed of three subunits, p150, p60, and p48, and is associated with the cellular DNA replication machinery through an interaction with PCNA, a sliding clamp for DNA polymerases, allowing the DNA replication-coupled deposition of histones (40, 41, 50). On the other hand, HIRA was identified as a DNA synthesis-independent histone chaperone in cell-free systems using *Xenopus laevis* egg extracts (32), and histone variant H3.3 was shown to mark transcriptionally active genomic regions (1). Furthermore, additional H3.3-specific chaperones were recently identified. Daxx is one of the components of promyelocytic leukemia (PML) nuclear bodies and was reported to deposit histone H3.3 onto specific genomic regions, such as telomeres and pericentric heterochromatin, together with an ATP-dependent chromatin remodeler, ATRX (10, 21). It was also reported that in *Drosophila melanogaster* cells, DEK is a coactivator of a nuclear receptor and functions as an H3.3-specific chaperone (37). Thus, the mechanistic evidences for histone deposition are accumulating in the case of cellular chromatin.

The regulatory events for the chromatin structure are not limited to the cellular genome, as some viruses also have chromatin and/or chromatin-like structures with their own genomes. The adenovirus (Ad) genome is a linear double-stranded DNA (dsDNA) of ~36,000 bp in length. In the virion, the Ad genome forms a chromatin-like structure with viral basic core proteins, as revealed by electron microscopic analyses showing that viral core protein-DNA complexes purified from the virion show a "beads-on-a-string" structure (49). Among core proteins, protein VII is a major DNA binding protein that can introduce superhelical turns into DNA, as do cellular histones (4), and remains associated with viral DNA after nuclear import of the virus genome (7, 17). When viral DNA-core protein complexes purified from the virion are used as a template for cell-free DNA replication/transcription systems, the reactions occur at a much lower level than in the case of naked DNA, indicating that the viral chromatin-like structure must be remodeled to execute its genome functions (22, 23). Pre-

Received 14 February 2012 **Accepted** 3 April 2012
Published ahead of print 11 April 2012
Address correspondence to Kyosuke Nagata, knagata@md.tsukuba.ac.jp.

doi:10.1128/JVI.00380-12